Proceedings of the 9th International Conference on Structural Dynamics, EURODYN 2014
Porto, Portugal, 30 June - 2 July 2014
A. Cunha, E. Caetano, P. Ribeiro, G. Müller (eds.)
ISSN: 2311-9020; ISBN: 978-972-752-165-4

Vibration-based damage identification of an unreinforced masonry house model

Claudio Oyarzo-Vera[1], Jason M. Ingham[2], Nawawi Chouw[2]
[1]Departamento de Ingeniería Civil, Universidad Católica de la Santísima Concepción, Concepción, Chile.
[2]Department of Civil and Environmental Engineering, University of Auckand, Auckland, New Zealand.
email: coyarzov@ucsc.cl, j.ingham@auckland.ac.nz, n.chouw@auckland.ac.nz

ABSTRACT: An unreinforced masonry house model was dynamically loaded using eccentric-mass shakers, with structural damage initiated by increasing the amplitude of the shaker load applied. At each damage state, a modal test was performed by impacting the house using a calibrated hammer. The structure's dynamic properties were extracted by Stochastic Subspace Identification techniques. Finally, two vibration-based damage indicators were applied to detect and determine the spatial distribution of damage, i.e. modal frequency variation and modal assurance criteria. It was concluded that prior to identifying the damage distribution, it was necessary to determine how the modal frequencies were related to each wall. Based on that individual wall information, only a rough identification of damage distribution can be achieved.

KEY WORDS: Unreinforced masonry, damage identification, impact test, modal analysis..

1 INTRODUCTION

Damage has been defined as a change that adversely affects the current or future performance of a system. Damage is usually related to structural responses that cause material non-linearity. However, the effect of damage is not only observed in post-elastic behaviour of structures because the linear response might also be perturbed due to degradation of elastic stiffness, loss of mass, or changes in the system boundary conditions.

A number of non-destructive techniques have been developed in the last three decades to detect damage beyond human naked-eye capacities (e.g. acoustic emissions, ultrasonic emissions or X-ray inspections). Most of these methods focus on assessing the local condition of structural elements, and they require a prior localization of the damage and access to the damaged area. Nevertheless, there are other kinds of non-destructive methods that can provide global information about damage in a structure. Global damage identification methods are, in general, based on the observation of changes in the dynamic response of structures, for example: modal frequency, mode shapes, modal curvatures and frequency response functions . Assuming that ambient conditions do not significantly affect the system properties, changes in the dynamic response can be associated with alteration of the mass, stiffness and damping matrices. Consequently, they can be interpreted as a symptom of structural damage. The main hypothesis of global damage identification is that an observation of variation in the elastic response of a system (modal properties) is sufficient to diagnose damage. Therefore, it is not necessary to force the structure into the non-linear range to verify damage.

The non-destructive nature of global damage identification techniques makes them especially attractive for localizing and assessing damage in structures of high historical and/or architectural value [1-4]. These techniques do not require direct access to the damaged zone, and thus they are particularly convenient from an economic and practical perspective, because damage can be detected early and "pre-localized". The information obtained by applying global damage identification techniques can then be used to decide whether a more detailed local analysis is necessary.

Most damage identification studies have focused on structures built using relatively homogeneous materials (e.g. steel and concrete). Only few studies have taken on the challenge of investigating damage in structures made of composite materials such as masonry (an assembly of bricks and mortar), with even fewer studies considering damage of heritage masonry buildings [5-7]

In our study, global damage identification methods based on vibration response were applied for detecting and roughly determining the spatial distribution of damage (damage localization) in an unreinforced masonry (URM) full-scale house model.

The house model was dynamically loaded using an eccentric-mass shaker placed on the roof diaphragm. Structural damage to the walls was initiated by increasing the amplitude of the load applied by the shaker. At different stages of damage, modal tests were performed by impacting the house using a calibrated hammer. The dynamic properties of the structure for the different damage states were extracted from the recorded accelerations by applying Stochastic Subspace Identification (SSI). Two simple vibration-based damage indicators (modal frequency variations and modal assurance criteria) were considered and applied to the results obtained from modal tests conducted on the URM house model. These indicators have been previously demonstrated to be effective in identifying damage in simple URM structural elements, such as cantilever wall panels [8].

2 HOUSE MODEL

An unreinforced clay brick masonry house model was constructed by an independent mason with deliberately minimal intervention by the analyst, with the aim of best replicating the typical construction practice used in New

Zealand for the construction of URM buildings between approximately 1880 and 1935 [9]. The specimen was built using recycled clay bricks obtained from demolition sites of old masonry buildings in Auckland, New Zealand. The mortar used to assemble the walls was lime based and had a cement : lime : sand ratio equal to 1 : 2 : 9. The use of this mortar mix has been shown to be appropriate for replicating the in-situ characteristics of historic unreinforced clay brick masonry buildings in New Zealand. The masonry compressive strength and Young's modulus were determined by standardized three-brick prism compressive tests [10], and were 3.9 MPa and 0.71 GPa, respectively.

The house dimensions were 4 m × 4 m in plan. The north, east and west walls had a height of 2.2 m and a thickness of 230 mm (two leaves of bricks), whereas the south wall had a height of 1.9 m and was 110 mm thick (one leaf of bricks). The bricks followed a common bond pattern (header course at every fourth course). The east and west walls had one opening for windows and the north wall had two openings for a window and a door. There were no openings in the south wall. A general view of the house model is shown in Figure 1.

A timber floor diaphragm that consisted of six equally spaced joists (45 mm × 140 mm) supported by the interior leaf of the east and west walls was located at a height of 1.60 m. These joists were connected by four equally spaced lines of blocking (45 mm × 140 mm). The diaphragm flooring was constructed over the joists using timber boards (32 mm × 140 mm) covered by 12 mm plywood sheets simulating a retrofit solution typically applied to floor diaphragms in New Zealand (Figure 2).

Figure 1. General view of the house model.

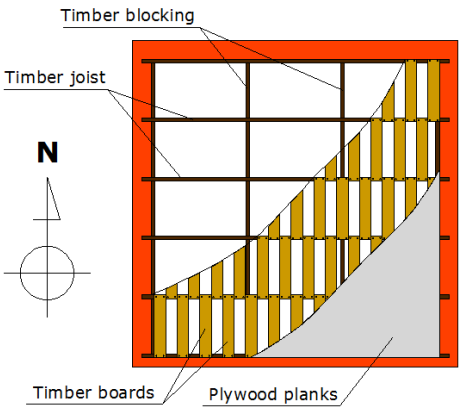

Figure 2. Timber diaphragm layout.

3 DYNAMIC EXCITACION CAUSING DAMAGE

The unreinforced masonry house model was dynamically tested with the aim of determining the effect of damage on the modal response of the structure. An eccentric-mass shaker (ANCO MK-140-10-50) attached to the roof diaphragm was used to damage the structure (Figure 3). The purpose of using a shaker to damage the house model was to produce a random, but controlled, deterioration that could then be detected by the damage identification procedures under investigation.

Four horizontal harmonic excitation sequences (ES1 to ES4) were applied by the shakers to the structure in the north-south direction. Within each excitation sequence, the magnitude of the excitation was gradually increased up to a maximum load (F_{max}) in a certain time-span (duration), as given in Table 1.

Figure 3. Eccentric mass shaker attached to the diaphragm.

Table 1. Damage State (DS) and excitation sequences (ES).

Damage State	Excitation Sequence	F_{max} (kN)	Duration (sec)
DS0			
	ES1	4.9	120
DS1			
	ES2	4.9	120
DS2			
	ES3	10.4	180
DS3			
	ES4	10.4	180
DS4			

3.1 Observed damage

The first excitation sequence (ES1) produced no visible damage (DS1). However, an excessive and undesired vertical deformation was observed in the diaphragm. This deformation originated in an overturning moment by the shaker, which produced a detachment of the floor boards and plywood sheets from the joists. This detachment affected the transference of load from the shaker, through the diaphragm, to the walls. To prevent this floor detachment, two box-section steel joists were added to the diaphragm in the north-south direction. These members were placed at the top of the diaphragm and firmly bolted to the timber joists below the diaphragm. The

addition of the steel joists significantly reduced the vertical deformation of the diaphragm during the second excitation sequence (ES2), but did not eliminate that deformation completely.

As no visible damage was observed at DS2, it was decided to increase the magnitude and duration of the next excitation sequence (ES3) to 10.4 kN and 180 seconds, respectively. As expected, significant and visible damage was generated in the specimen (DS3). In the south wall, a long horizontal crack at the diaphragm level was observed (Figure 4a) and diagonal cracks around the door opening were detected in the north wall. Also, several cracks were detected at the upper corners of the walls. These cracks were related to out-of-plane failure of the parapet (Figures 4b and 4c).

The final excitation sequence (ES4) produced severe damage, especially in the north and south walls (DS4). In the south wall, the two upper brick courses fell down and diagonal cracks typical of wall out-of-plane failure were developed (Figure 5a). The parapet of the north wall was heavily damaged, even losing some bricks. The cracks around the door and window openings that had been previously detected now became wider and new cracks were also identified (Figure 5b). Cracks were noticed around the window openings of the east and west walls, but the most significant damage was observed in the upper corners of those walls, probably because of the effect of the out-of-plane failure of the north and south walls (Figures 5c and 5d).

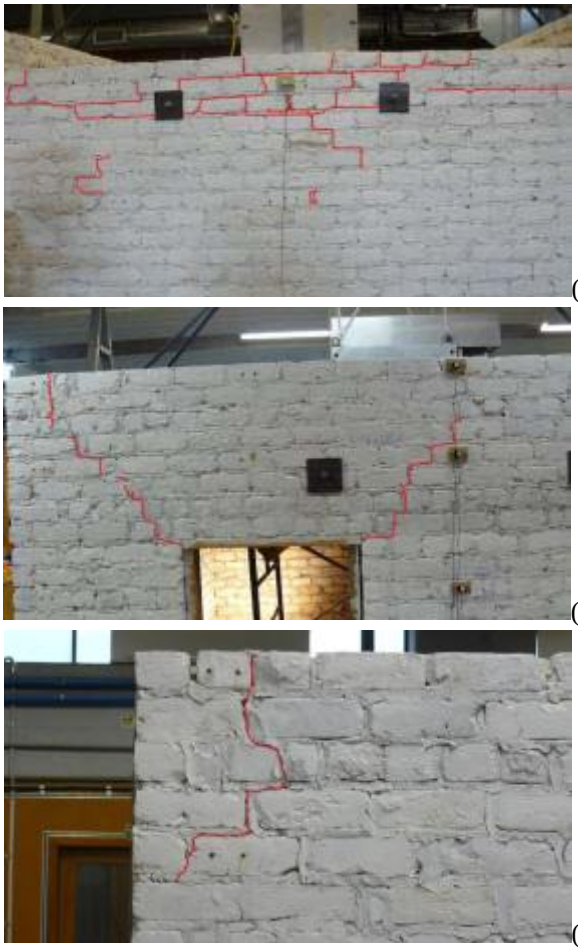

(a) (b) (c)

Figure 4. Damage observed at DS3. (a) South wall, (b) North wall, and (c) North-west walls' corner

(a) (b) (c) (d)

Figure 5. Damage observed at DS4. (a) South wall, (b) North wall, (c) North-west walls' corner, and (d) Soutth-west walls' corner

4 MODAL TEST

Modal tests were conducted before loading the structure (DS0) and after each excitation sequence to determine the dynamic properties of the structure (modal frequencies and mode shapes) at different states of damage (DS1 to DS4). The modal tests consisted of exciting the structure by impacts with a calibrated hammer (Dytran 5803A) and recording the vibration response using accelerometers (Crossbow CXL02LF1Z and CXL10HF1Z). A total of six hits per wall was applied, two at each of the locations (H1, H2 and H3) as indicated in Figure 6. The structural response was recorded for 30 seconds at a sample rate of 500 readings per second in the direction normal to the wall face over a grid of 20 measure points per wall, as also displayed in Figure 6.

Data acquisition was conducted using a 48-channel signal conditioning box that amplified the signals to the range of +/- 10 V. This equipment was connected to a 16-bit Analog Data Acquisition and Control Cube manufactured by United Electronics Industries (DNA-PPC5). The system was controlled by a Matlab code developed by the first author. A 5th order Butterworth low-pass filter was applied, with a 200 Hz cut-off frequency.

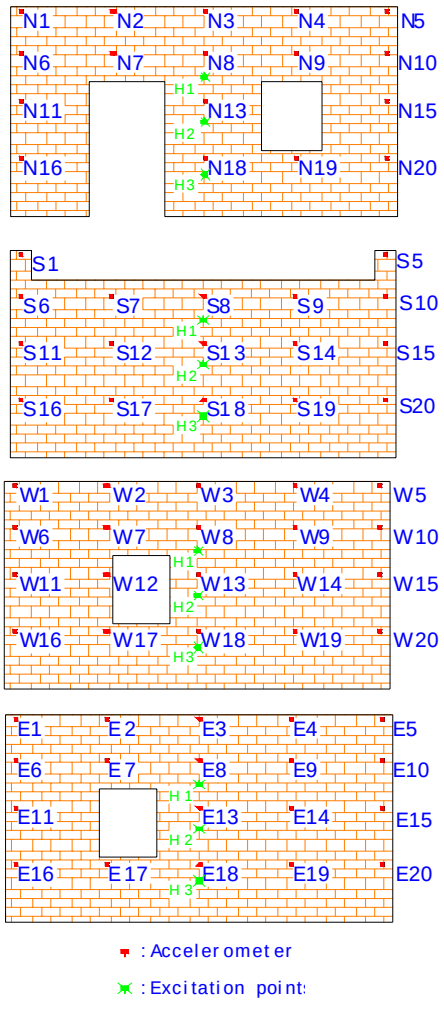

Figure 6. Measurement grid and excitation points. (a) North wall, (b) South wall, (c) West wall, and (d) East wall

Stochastic Subspace Identification (SSI) was used for extracting the modal properties from the recorded data. The SSI method has been shown to provide good performance in previous experiments conducted by our research group and others [11-13]. The SSI algorithm was applied to every independent impact test, with 18 tests per wall (72 tests in total).

4.1 Modes identification

It was observed that different modes were generally related to the response of specific parts of the building (walls or diaphragm response). Nevertheless, there were several frequencies detected in multiple walls that were associated with a global system response or corresponded to the response of other parts of the structure indirectly excited by the impact. The modal frequencies identified by the SSI method are shown in Table 2.

Recognising that no damage was observed in the structure due to the first excitation sequence (ES1), it would be expected that no major difference in building condition should be detected between the results of DS0 and DS1. Nevertheless, minor system alterations might be anticipated, because of the "self-adjustment" or "settlement" of the structural components during ES1. This situation was reflected in the results presented in Table 2 for DS0 and DS1, where the same set of six modal frequencies was detected in both damage states.

The modal frequency labelled as Freq. 3 was clearly identified in all walls at approximately 17 Hz. It was difficult to determine if this response was related to one particular wall, because the wall-diaphragm connectors tied all walls together and increased the interaction between the different structural members. Nevertheless, considering the results obtained from previous experiments [12] and the response recorded at higher levels of damage (DS3 and DS4), it was assumed that Freq. 3 was effectively related to a modal response with an important participation of the south wall.

Freq. 4 was detected at approximately 20 Hz. This mode was related to a north-south response of the structure. Again, the inclusion of wall-diaphragm connectors contributed to a transfer of the response of north wall, through the diaphragm, to the south wall.

Freq. 6 was related to another mode with a significant participation of the north wall (at approximately 36 Hz) which was also detected in the east and west walls.

Freq. 7 and Freq. 8 corresponded to twin-modes associated with the west and east walls, respectively. Under ideal conditions the frequency and mode shapes of these twin-modes would be completely identical. The difference observed between these modes was attributed to potential dissimilarities in material properties, support conditions and construction quality. Another east wall mode was detected at approximately 44 Hz (Freq. 9).

As described in section 3.1, two steel joists were used to reinforce the diaphragm after DS1 with the aim of reducing the vertical deformation due to the overturning moment generated by the shaker. This intervention in the structure was considered as a retrofit that altered the system baseline conditions. To conduct the most appropriate analysis, DS2 was considered as a reference condition for examination of the subsequent states of damage. The reference state DS2

considered a system configuration that included the diaphragm reinforcement and a relatively low level of damage generated by the low magnitude excitation sequences ES1 and ES2. This new configuration contributed to the generation of the eight modal frequencies associated with the new reference condition DS2.

Freq. 2 corresponded to a mode at approximately 13 Hz, mainly associated with a response of the east and west walls. That mode was not detected in the previous damage states before reinforcing the diaphragm.

Freq. 3 was detected for DS2 at 17 Hz. This mode was also detected at DS0 and DS1 and was associated with the south wall response. In the case of DS2, the link between this mode and the south wall was confirmed. The frequency was also identified at DS3, but at 16.2 Hz.

Freq. 4 was detected in the north wall at 20 Hz, similar to the results obtained for DS0 and DS1. This frequency disappeared in the subsequent states of damage (DS3 and DS4). For DS4, a frequency of approximately 19.5 Hz was detected in the east and west walls, but the correspondence of that frequency to the mode previously detected in the north wall was not completely clear.

Freq. 5 was not identified in DS0 and DS1, but was clearly detected in DS2 and the subsequent states of damage. This mode had a frequency of approximately 24 Hz and was related to a modal response dominated by east wall vibration.

Freq. 6, of approximately 36.5 Hz, was related to a modal response of the east and west walls. In the previous states of damage, this frequency was related to a mode with a predominant participation of the north wall. Freq. 7 and Freq. 8 (of approximately 38.5 Hz and 40 Hz, respectively) were related to modal responses with strong participation of the south and north walls, respectively. Before the diaphragm was reinforced, Freq. 7 and Freq. 8 were related to a response dominated by vibration of the west and east walls, respectively. Hence, it was interpreted that the intervention in the diaphragm generated a "swap" in the modes associated with Freq. 6, Freq. 7 and Freq. 8.

Freq. 9 was related to a response of the east wall at approximately 44 Hz, similar to that observed before reinforcing the diaphragm.

Once severe damage was generated in the structure (DS3 and DS4), another low frequency mode was detected at approximately 11 Hz (Freq. 1). This mode was interpreted as a result of rocking or cantilever vibration of the parapets that had lost their lateral supports due to damage. However, this interpretation was only intuitive and no measured data was available to confirm this assumption.

5 VIBRATION BASED DAMAGE IDENTIFICATION

The relationship observed between degradation of structural properties (stiffness and mass) and changes in modal frequencies was a main promoter for developing vibration-based damage identification techniques. Because frequency measurements can be quickly conducted and have a lower data scatter than do mode shapes and damping measurements, damage parameters related to modal frequencies have historically been preferred [14]. In the study presented here, statistically significant variations of the modal frequencies, calculated before and after damage was introduced, were employed to detect damage.

The change in mode shapes detected before and after damage was generated was employed as a damage indicator. The difference in mode shapes can be generated by stiffness degradation, change in the mass distribution, and alterations in the system geometry and boundary conditions. The Modal Assurance Criteria (MAC) is an indicator that quantifies the degree of similarity between two mode shape vectors (Eq. 1), and is therefore used to detect differences between mode shapes measured before and after damage. Previous studies [15] have confirmed that a good result can be achieved, even in the case when frequency-based indicators were not able to identify structural deterioration. The equation that defines MAC is:

$$MAC_j = \frac{\left(\{\phi_j^0\}^T \cdot \{\phi_j^D\}\right)^2}{\left(\{\phi_j^0\}^T \cdot \{\phi_j^0\}\right) \cdot \left(\{\phi_j^D\}^T \cdot \{\phi_j^D\}\right)} \quad (1)$$

where $\{\phi_j^0\}$ and $\{\phi_j^D\}$ correspond to the mode shape vectors of the j^{th} mode for the undamaged and damaged condition, respectively.

Both damage indicators (statistically significant variation of modal frequency and Modal Assurance Criteria) were employed to identify damage in the house model. The effectiveness of the above introduced indicators to identify damage in URM structures under ideal conditions (e.g. homogeneous properties of bricks and mortar and perfect connection at the brick-mortar interface) was successfully demonstrated in preliminary tests using numerical simulations and in physical tests on simple URM structures [8].

5.1 Damage identification results

Three study cases were analysed: (i) structural dynamic behaviour before reinforcing the diaphragm with steel joists (DS0 vs. DS1); (ii) the effect of reinforcement of the diaphragm on the dynamic behaviour (DS1 vs. DS2); and (iii) the effect of damage on the dynamic behaviour of the structure with the reinforced diaphragm (DS3 and DS4 compared to DS2). In each of these cases, only those modes detected in the reference damage state and in at least one of the subsequent damage states were considered, and the response of every wall was considered independently. Those modes that were not detected in the reference damage state (new modes generated by damage or structural modification) were omitted in this analysis.

The frequency based analysis was conducted considering that the database was normally distributed. Hypothesis tests considering a 95% confidence were applied to determine whether corresponding frequencies detected at different states of damage were statistically different or similar. Summaries of these results for each study case are shown in Tables 3 to 5. These tables display the frequencies detected at the reference damage state, the percentage variation of these frequencies relative to the reference condition, and a label ("Yes" or "No") to indicate whether or not this variation is statistically significant.

The MAC factors computed for each wall and for the different study cases are presented in Figures 7 to 10.

Table 2. Modal frequencies (Hz) detected in the specimen

	Wall	DS0 Average (CoV)	DS1 Average (CoV)	DS2 Average (CoV)	DS3 Average (CoV)	DS4 Average (CoV)
Freq. 1	**North**				11.875 (5%)	--
	South				11.600 (5%)	--
	East					10.664 (3%)
	West					10.824 (3%)
Freq. 2	**North**					--
	South					--
	East			13.602 (2%)	13.645 (3%)	12.265 (8%)
	West			13.876 (4%)	13.260 (1%)	14.354 (6%)
Freq. 3	**North**	18.250 (1%)	17.203 (3%)			--
	South	17.598 (1%)	16.857 (2%)	16.906 (2%)	16.670 (3%)	--
	East	17.536 (1%)	17.222 (2%)	17.640 (4%)	16.867 (5%)	
	West	17.380 (1%)	17.309 (1%)	17.065 (1%)	16.189 (1%)	
Freq. 4	**North**	20.953 (1%)	19.767 (2%)	20.267 (3%)		--
	South	19.203 (2%)	19.244 (3%)			--
	East					19.668 (3%)
	West					19.552 (3%)
Freq. 5	**North**				24.657 (4%)	--
	South					--
	East			25.792 (1%)	25.092 (1%)	25.050 (1%)
	West				24.667 (2%)	
Freq. 6	**North**	36.623 (1%)	36.251 (2%)			--
	South					--
	East		36.066 (1%)	37.098 (1%)	37.278 (1%)	
	West		35.106 (1%)	36.792 (1%)	36.038 (3%)	
Freq. 7	**North**	38.878 (1%)				--
	South			38.987 (1%)	38.285 (2%)	--
	East					
	West	38.668 (1%)	38.714 (1%)			
Freq. 8	**North**			41.203 (1%)	40.491 (2%)	--
	South		40.611 (2%)			--
	East	39.995 (1%)	39.558 (1%)		39.248 (1%)	
	West					
Freq. 9	**North**					--
	South					--
	East	44.462 (1%)	43.814 (1%)	43.907 (1%)	42.202 (1%)	42.837 (1%)
	West	43.992 (1%)				

Note: In the case of DS4, no information is presented for the north and south walls, because the response was not measured in those walls due to their severe deterioration at this state of damage.

In the case of the structure analysed before the diaphragm was reinforced with two box-section steel joists (DS0 vs. DS1, see Table 3), statistically significant frequency reduction was observed in several modes, especially in the walls that had the most important participation in the corresponding mode. The most significant frequency reductions for Freq. 3 and Freq. 4 occurred in the south and north walls, respectively. Significant frequency drops were also detected in Freq. 8 and Freq. 9. Both associated with a mode principally recorded in the east wall. The observed frequency degradation was explained by a general degradation (softening) of materials that did not necessarily manifest itself as visible cracks. This general degradation in stiffness did not affect particular sections of the system or alter the boundary conditions. Therefore, the relative magnitudes of modal displacements within the mode shape vectors measured before and after damage were not altered, as can be inferred from the relatively high MAC values computed for this case (Figure 7).

The results of the analyses that compared the structure before and after reinforcing the diaphragm with two steel joists (DS1 vs. DS2) are presented in Table 4. This case also considered the effect of the small magnitude excitation ES2. Statistically significant increments of the modal frequencies were observed in Freq. 4 and Freq. 6. This frequency rise was related to a restitution of stiffness due to reinforcement of the diaphragm. An exception to this behaviour was observed in the west wall for Freq. 3, in which modal frequency dropped. However, participation of the west wall was secondary in this mode. The changes observed in the modal frequencies support the decision to consider DS2 as the reference condition in the subsequent analysis, because the degradation due to the loads applied (ES1 and ES2) and the structural intervention (diaphragm reinforcement) modified the reference baseline. Similar to the situation observed in the previous study case (DS0 vs. DS1), the MAC values computed for each wall were high (Figure 8), except for the case of the south wall where no reliable modes to calculate MAC were identified. The high MAC values showed an elevated level of correspondence between the mode shapes of DS1 and DS2, probably because no damage was produced in the walls to generate a variation in the relative magnitudes of the modal displacements within the mode shape vectors.

The large magnitude load sequences (ES3 and ES4) produced a significant reduction in most of the modal frequencies (Table 5), except for Freq. 7. It is noted that Freq. 2 and Freq. 5 corresponded to modes detected after the inclusion of the steel joists used to reinforce the diaphragm. For the case of DS3 compared to DS2 (Figure 9), damage was also detected by the MAC in all the walls (MAC < 85%), with the effect being more accentuated in the north wall which

coincided with the damage observed in the experiment. A less significant difference was observed in the south wall (MAC = 83%), which was explained by the damage concentrated at the top of the wall and almost insignificant damage in the rest of the panel. The differences observed in the east and west walls were attributable to indirect effects of the damage in the north and south walls. The MAC factors calculated for the case of DS4 compared to DS2 (Figure 10) were also affected by damage; however, the results were not totally consistent with the damage progression. MAC decreased in the east wall, while it increased in the west wall.

Table 3: Modal frequency variation before reinforcing the diaphragm (DS1 relative to DS0)

		DS0 vs DS1	
	Wall	**Freq. Var.**	**Signif. Var.**
Freq. 3	North	-5.7	No
	South	-4.2%	Yes
	East	-1.8%	Yes
	West	-0.4%	No
Freq. 4	North	-5.7%	Yes
	South	0.2%	No
	East		
	West		
Freq. 6	North	-1.0%	No
	South		
	East		
	West		
Freq. 7	North		
	South		
	East		
	West	0.1%	No
Freq. 8	North		
	South		
	East	-1.1%	Yes
	West		
Freq. 9	North		
	South		
	East	-1.5%	Yes
	West		

Table 4: Effect of the diaphragm reinforcement in the modal frequencies (DS2 relative to DS1)

		DS1 vs. DS2	
	Wall	**Freq. Var.**	**Signif. Var.**
Freq. 3	North		
	South	0.3%	No
	East	2.4%	No
	West	-1.4%	Yes
Freq. 4	North	2.5%	Yes
	South		
	East		
	West		
Freq. 6	North		
	South		
	East	2.9%	Yes
	West	4.8%	Yes
Freq. 9	North		
	South		
	East	0.2%	No
	West		

Table 5: Modal frequency variation after reinforcing the diaphragm (DS3 and DS4 relative to DS2)

		DS2 vs. DS3		DS2 vs. DS4	
	Wall	**F. Var.**	**S. Var.**	**F. Var.**	**S. Var.**
Freq. 2	North			--	
	South			--	
	East	0.3%	No	-9.8%	No
	West	-4.4%	Yes	3.4%	Yes
Freq. 3	North			--	
	South	-1.4%	No	--	
	East	-4.4%	No		
	West	-5.1%	Yes		
Freq. 5	North			--	
	South			--	
	East	-2.7%	Yes	-2.9%	Yes
	West				
Freq. 6	North			--	
	South			--	
	East	0.5%	No		
	West	-2.0%	Yes		
Freq. 7	North			--	
	South	-1.8%	No	--	
	East				
	West				
Freq. 8	North	-1.7%	Yes	--	
	South			--	
	East				
	West				
Freq. 9	North			--	
	South			--	
	East	-3.9%	Yes	-2.4%	Yes
	West				

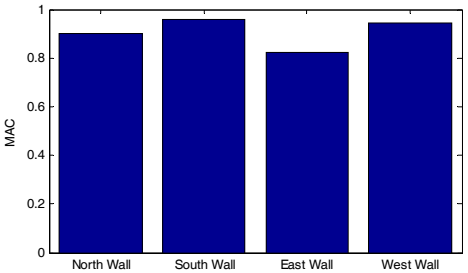

Figure 7. MAC obtained for the results of DS1 vs. DS0

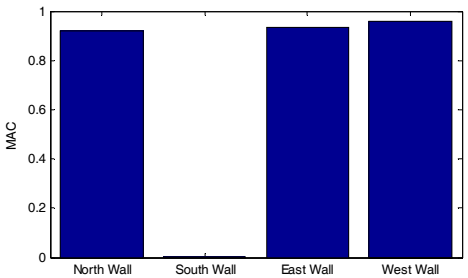

Figure 8. MAC obtained for the results of vs. DS1

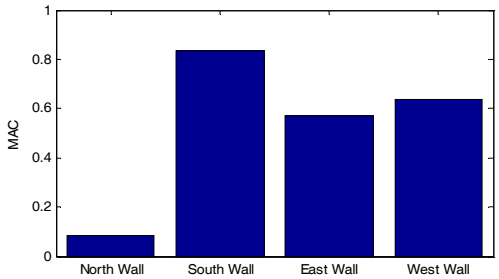

Figure 9. MAC obtained for the results of DS3 vs. DS2

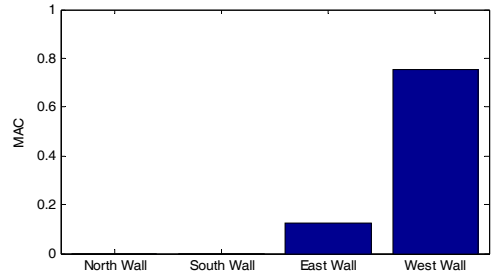

Figure 10. MAC obtained for the results of DS4 vs. DS2

6 CONCLUSIONS

None of the low magnitude excitation sequences (ES1 and ES2) generated visible damage. However, a decrement of the most predominant frequency (Freq. 3) was observed in all walls, which was attributed to a generalized degradation of stiffness (material softening). The detection of such system alterations at early states of damage was considered an advantage of the method, because changes in this modal frequency might potentially be used as a damage indicator. Unfortunately, although the frequency drop observed in Freq. 3 persisted in the subsequent states of damage (DS3 and DS4), it was not always statistically significant.

The large magnitude excitations (ES3 and ES4) produced statistically significant frequency drops in most modes. Nevertheless, the magnitude of the frequency variation was not always consistent with the severity of the damage observed. The most significant frequency variations were not associated with the most severely damaged walls.

A reduction in the MAC value was observed only when severe damage was generated (DS3 and DS4). When the damage was not manifested as cracks or any other phenomena that altered the mode shapes geometry (for example, change in boundary conditions), MAC was unable to detect damage. That case was observed for DS0 vs. DS1 and DS1 vs. DS2.

The relative severity of damage was not properly reflected by MAC. More severely damaged walls (for example the south wall) did not necessarily exhibit a smaller MAC than that of other walls that had experienced a milder damage (for example the east and west walls). Consequently, MAC can be used to detect severe damage, but it is ineffective for comparing the relative damage generated in each of the walls.

The evaluation of the two damage indicators revealed that it was not possible to identify the damage distribution based only on the global response. Instead, it was necessary to determine the response of each wall and how the frequencies were related to each wall (or group of walls). Based on the information collected for the individual walls, a rough identification of the spatial distribution of damage (the determination of which wall is damaged) can be achieved with acceptable levels of reliability.

ACKNOWLEDGEMENTS

The authors acknowledge the support of the New Zealand Foundation for Research, Science and Technology (Project UOAX0411) for this research program, and the support of the Chilean Government (Beca Presidente de la República) and the Universidad Católica de la Santísima Concepción (UCSC, Chile) that enabled the first author's doctoral studies in New Zealand.

REFERENCES

[1] Gentile, C. and A. Saisi, *Ambient vibration testing of historic masonry towers for structural identification and damage assessment.* Construction and Building Materials, 2007. **21**(6): p. 1311-1321.

[2] Ramos, L.F., L. Marques, P.B. Lourenço, G. De Roeck, A. Campos-Costa, and J. Roque, *Monitoring historical masonry structures with operational modal analysis: Two case studies.* Mechanical Systems and Signal Processing, 2010. **24**(5): p. 1291-1305.

[3] Durukal, E., S. Cimilli, and M. Erdik, *Dynamic response of two historical monuments in Istanbul deduced from the recordings of Kocaeli and Duzce earthquakes.* Bulletin of the Seismological Society of America, 2003. **93**(2): p. 694-712.

[4] Beyen, K., *Structural identification for post-earthquake safety analysis of the Fatih mosque after the 17 August 1999 Kocaeli earthquake.* Engineering Structures, 2008. **30**(8): p. 2165-2184.

[5] Ramos, L.F., P.B. Lourenco, G. De Roeck, and A. Campos-Costa, *Damage identification in masonry structures with vibration measurements*, in *Structural Analysis of Historic Construction: Preserving Safety and Significance, Vols 1 and 2*, D. Dayala and E. Fodde, Editors. 2008, Crc Press-Taylor & Francis Group: Boca Raton. p. 311-319.

[6] Ramos, L.F., G. De Roeck, P.B. Lourenço, and A. Campos-Costa, *Damage identification on arched masonry structures using ambient and random impact vibrations.* Engineering Structures, 2010. **32**(1): p. 146-162.

[7] Ramos, L.F., A. Campos-Costa, and P.B. Lourenço. *Operational modal analysis for damage detection of a masonry construction*. in *1st Int. Operational Modal Analysis Conference*. 2005. Copenhagen, Denmark.

[8] Oyarzo-Vera, C. and N. Chouw, *Vibration-based damage identification of an unreinforced masonry panel*, in *5th International Operational Modal Analysis Conference (IOMAC 2013)*2013: Guimaraes, Portugal.

[9] Russell, A. and J. Ingham, *Prevalence of New Zealand's Unreinforced Masonry Buildings.* Bulletin of the New Zealand Society for Earthquake Engineering, 2010. **43**(3): p. 182 – 201.

[10] ASTM C1314, *Standard test method for compressive strength of masonry prisms*. 2010 ed. Officials Standard, ed. A. International. 2010, West Conshohocken, PA, USA.: ASTM International.

[11] Ramos, L.F., *Damage identification on masonry structures based on vibration signatures*. 2007 PhD in Civil Engineering. Escola de Engenharia, Universidade do Minho, Portugal.

[12] Oyarzo Vera, C.A., *Damage identification of unreinforced masonry structures based on vibration response*. 2012 PhD in Civil Engineer. Department of Civil and Environmental Engineering, University of Auckland, New Zealand.

[13] Peeters, B., *System Identification and Damage Detection in Civil Engineering*. 2000. Departement Burgerlijke Bouwkunde, Katholike Universiteit Leuven, Heverlee, Belgium.

[14] Salawu, O.S., *Detection of structural damage through changes in frequency: a review.* Engineering Structures, 1997. **19**(9): p. 718-723.

[15] Doebling, S.W., C.R. Farrar, M.B. Prime, and D.W. Shevitz, *Damage identification and health monitoring of structural and mechanical systems from changes in their vibration characteristics: A literature review.*, 1996, Los Alamos National Laboratory: Los Alamos, New Mexico.